

# 1 Vertical profiles of sub-3 nm particles over the boreal forest

2

3 Katri Leino<sup>1\*</sup>, Janne Lampilahti<sup>1</sup>, Pyry Poutanen<sup>1</sup>, Riikka Väänänen<sup>1</sup>, Antti Manninen<sup>1</sup>, Stephany  
4 Buenrostro Mazon<sup>1</sup>, Lubna Dada<sup>1</sup>, Anna Franck<sup>1</sup>, Daniela Wimmer<sup>1</sup>, Pasi P. Aalto<sup>1</sup>, Lauri R.  
5 Ahonen<sup>1</sup>, Joonas Enroth<sup>1</sup>, Juha Kangasluoma<sup>1</sup>, Petri Keronen<sup>1</sup>, Frans Korhonen<sup>1</sup>, Heikki Laakso<sup>1</sup>,  
6 Teemu Matilainen<sup>1</sup>, Erkki Siivola<sup>1</sup>, Hanna E. Manninen<sup>1,2</sup>, Katrianne Lehtipalo<sup>1,3</sup>, Veli-Matti  
7 Kerminen<sup>1</sup>, Tuukka Petäjä<sup>1</sup> and Markku Kulmala<sup>1</sup>

8 <sup>1</sup> Institute for Atmospheric and Earth System Research / Physics, Faculty of Science, P.O. Box 64, FI-00014 University  
9 of Helsinki, Finland

10 (\* corresponding author's email: [katri.e.leino@helsinki.fi](mailto:katri.e.leino@helsinki.fi))

11 <sup>2</sup>CERN, CH-1211Geneva 23, Switzerland.

12 <sup>3</sup>Finnish Meteorological Institute, Erik Palménin aukio 1, 00560 Helsinki, Finland

13 **Abstract.** This work presents airborne observations of sub-3 nm particles in the lower troposphere  
14 and investigates new particle formation (NPF) within an evolving boundary layer (BL). We studied  
15 particle concentrations together with supporting gas and meteorological data inside the planetary BL  
16 over a boreal forest site in Hyytiälä, Southern Finland. The analysed data were collected during three  
17 flight measurement campaigns: May-June 2015, August 2015 and April-May 2017, including 27  
18 morning and 26 afternoon vertical profiles. As a platform for the instrumentation, we used a Cessna  
19 172 aircraft. The analysed flight data were collected horizontally within a 30-km distance from the  
20 SMEAR II station in Hyytiälä and vertically from 100 m above ground level up to 2700 m. The  
21 number concentration of 1.5–3 nm particles was observed to be, on average, the highest near the  
22 forest canopy top and to decrease with an increasing altitude during the mornings of NPF event days.  
23 This indicates that the precursor vapours emitted by the forest play a key role in NPF in Hyytiälä.  
24 During daytime, newly-formed particles were observed to grow in size and the particle population  
25 became more homogenous within the well-mixed BL in the afternoon. During undefined days in  
26 respect to NPF, we also detected an increase in concentration of 1.5–3 nm particles in the morning  
27 but not their growth in size, which indicates an interrupted NPF process during these undefined days.  
28 Vertical mixing was typically stronger during the NPF event days than during the undefined or non-  
29 event days. The results shed light on the connection between boundary layer dynamics and NPF.

30

# 31 1 Introduction

32

33 One of the most important sources of secondary aerosol particles in the atmosphere is new particle  
34 formation (NPF). NPF and subsequent growth is a globally observed phenomenon (Kulmala et al.,  
35 2004; Kulmala and Kerminen, 2008; Kerminen et al., 2018). It is still partly unclear where, when and  
36 how NPF occurs in the atmosphere. Aerosol measurements on board of an aircraft can give  
37 information about the vertical, horizontal and spatial extent of the NPF in the lower atmosphere.

38 The planetary boundary layer (PBL) is a complex layer in the lowest part of the atmosphere, defined  
39 as the part of the troposphere that is directly connected to the Earth's surface through the exchange  
40 of momentum, heat and mass, and responds to surface forcing with a timescale of an hour or less  
41 (Stull, 2012). The PBL has a characteristic diurnal cycle, but the detailed development varies from  
42 day to day. Several meteorological, physical and chemical processes influence the spatial and  
43 temporal conditions inside the BL and thus the mixing strength and evolution of boundary layer. This  
44 gives rise to the complexity to define the exact BLH or to characterize the typical BL structure or  
45 height at a given location.

46 Several airborne measurements have been conducted to investigate particle number concentrations  
47 and size distributions as well as NPF inside the PBL. Over Europe, Crumeyrolle et al. (2010) observed  
48 that the horizontal extent of NPF was about 100 km or larger during the EUCAARI campaign in 2008  
49 (Kerminen et al., 2010), while Wehner et al. (2007) estimated a corresponding scale of up to 400 km  
50 with clear horizontal variability in NPF characteristics during the SATURN campaign in 2002. The  
51 number concentrations and size distributions of naturally charged particles (air ions) were under  
52 investigation during EUCAARI-LONGREX campaign in May 2008 (Mirme et al., 2010). They  
53 reported that NPF takes place throughout the whole BL, and that the particles have formed more  
54 likely via neutral than ion-induced pathways inside the PBL.

55 One of the sinks of newly formed aerosol particles in the PBL is dry deposition, which is important  
56 especially for the smallest particles (Rannik et al., 2000; Lauros et al., 2011). Recently, Zha et al.  
57 (2018) studied the vertical profile of highly oxygenated organic compounds (HOMs), which are  
58 known precursors for aerosol formation (Ehn et al., 2014). They found that while the concentrations  
59 were similar below and above canopy (35 m) during well-mixed conditions, the concentrations were  
60 often clearly lower near the ground level during night-time, when temperature inversion occurred,  
61 probably due to changes in their sources and sinks (e.g. surface deposition) during stable conditions.

62 In addition to NPF near to the surface inside the PBL and NPF in the free troposphere (FT) (Bianchi  
63 et al., 2016), NPF has also been observed near clouds (Wehner et al., 2015). Siebert et al. (2004),  
64 Platis et al. (2016) and Chen et al. (2018) observed NPF to initiate on top of the boundary layer in a  
65 capping inversion followed by subsequent mixing of the freshly formed particles throughout the well-  
66 mixed boundary layer. Wehner et al. (2010) studied NPF in the residual layer and observed that  
67 turbulent mixing is likely to lead to a local super saturation of possible precursor gases, which is  
68 essential for NPF. The particles were formed in parts of the residual layer and subsequently entrained  
69 into the BL where they were detected at the surface.

70 NPF events are frequently occurring over the boreal forest region in Southern Finland (Kulmala et  
71 al., 2001; Dal Maso et al., 2005; Kulmala et al., 2013). In addition to ground-based measurements at  
72 the SMEAR II station (61°51'N, 24°17'E, 181 m above sea level, Hari and Kulmala, 2005), which  
73 have been conducted continuously since 1996, also airborne measurements of aerosol particles have  
74 been carried out near the station since the year 2003 during several campaigns using a small aircraft  
75 (O'Dowd et al., 2009; Schobesberger et al., 2013) and a hot-air balloon (Laakso et al., 2007). Laakso  
76 et al. (2007) observed NPF to occur in the mixed BL, but also in the FT with no connection to the BL  
77 nucleation. O'Dowd et al. (2009) observed NPF throughout the BL over the SMEAR II, with the  
78 nucleation mode number concentration peaking first above the forest canopy. Schobesberger et al.  
79 (2013) observed NPF inside the PBL. High concentrations of nucleation mode particles were also  
80 found in the upper parts of the PBL, which indicates that nucleation does not necessarily occur only  
81 close to the surface. The vertical profiles of small particles in mixing BL at SMEAR II were also  
82 modelled by Boy et al. (2006). Their results predicted that the maximum of newly formed clusters  
83 and particle concentrations is located near the ground level.

84 In this study, we investigate the vertical variation of 1.5–3 nm and 3–10 nm particles from the ground  
85 level up to 3 kilometres during different kind of days in relation to the occurrence of NPF at the  
86 ground level, as well as the vertical mixing of a particle population within the evolving BL. The  
87 dataset was collected during three measurement flight campaigns, in spring 2015, August 2015 and  
88 in spring 2017, within a 30-km distance from the SMEAR II station. The results are compared to the  
89 data measured on the ground level at the station. Traditional NPF event classification is used to  
90 classify studied days as NPF events, non-events and undefined days (Dal Maso et al., 2005).

91 The questions we would like to answer are: Which kind of characteristics do we have in the vertical  
92 profile of small particles?; How do these profiles differ between the NPF event, non-event and  
93 undefined days?; Where do new particles form and how does the strength of turbulent mixing affect

94 particle concentrations?; What is the median concentration of small particles inside the BL during the  
95 NPF event, non-event and undefined days, and how well do the results agree with the values measured  
96 on the ground level?

97

## 98 **2 Materials and methods**

### 99 **2.1 Measurements on board Cessna**

100 As a platform for aerosol instruments, we used a light one-engine Cessna FR172F aircraft. The  
101 measurement instruments were installed on an aluminium rack at the middle part inside the plane's  
102 cabin (Fig. 1). A steel inlet line (with 32 mm inner diameter) was mounted onto the top of the rack  
103 and lifted in and out from the window in the left side of the plane. The sample was collected from a  
104 50-cm distance from the fuselage of the plane. The main flow in the steel tube was kept constant at  
105  $47 \text{ l min}^{-1}$  during the measurement flight and was produced by suction in the venturi and forward  
106 motion of the airplane. Each instrument took their actual inlet flow from the central line of the main  
107 flow, minimizing the diffusional losses of the smallest particles. The measurements were performed  
108 with an airspeed of 125 km/h. More details about partly the same instrumentation and layout can be  
109 found in Schobesberger et al. (2013) and Väänänen et al. (2016). The data were collected within a  
110 30-km distance from SMEAR II station and the area is covered mainly by coniferous forest.

#### 111 **2.1.1 Instrumentation**

112 The main instrumentation for this study consisted of several different particle counters. An ultrafine  
113 condensation particle counter (uCPC, model TSI-3776) is an instrument that detects the total  
114 concentration of particles larger than about 3 nm in diameter. Particles larger than the threshold  
115 diameter are grown into large droplets by condensing butanol vapour onto their surface, after which  
116 they are detected optically with a laser-diode photodetector. The ultrafine CPC has an internal vacuum  
117 pump that draws the aerosol sample with flow rate of  $1.5 \text{ l min}^{-1}$  into the instrument.

118 Airmodus Ltd has developed a mixing-type Particle Size Magnifier (PSM). The instrument is able to  
119 detect directly sub-3 nm atmospheric particles using diethylene glycol (DEG) as condensing fluid  
120 (Vanhanen et al., 2011). Compared with typically-used working fluids in CPCs, water and butanol,  
121 the advantages of using DEG as condensing fluid are its lower saturation vapour pressure and higher  
122 surface tension, which enables to detect particles down to 1 nm. The PSM requires a separate water  
123 or butanol counter (CPC) for detecting optically the grown particles. The PSM in this study was a  
124 model A10, operating with a butanol CPC (model TSI-3010). During the flight measurements

125 presented here, the instrument was used in fixed saturator flow rate mode measuring the total particle  
126 concentration with a 1.5 nm cut-off size.

127 The instrumentation included also a custom-built Scanning Mobility Particle Sizer (SMPS), which  
128 measures the particle number size distribution in the diameter size range of 10–400 nm with a 2-min  
129 time resolution. Before the classification of an aerosol population, the particles are transported to a  
130 radioactive source where they reach a constant bipolar charge equilibrium. The SMPS contains a  
131 differential mobility analyser (DMA, Hauke type), while particle number concentrations are  
132 measured with a butanol CPC (model TSI-3010).

133 The concentrations of water vapour (H<sub>2</sub>O) and carbon dioxide (CO<sub>2</sub>) were measured with a Li-Cor  
134 (LI-840) gas analyser located in the instrumentation rack. Basic meteorological variables, including  
135 the ambient temperature (with PT-100 temperature sensor), relative humidity (RH) (with Rotronic  
136 HygroClip-S sensor) and static pressure (with Vaisala PTB100B), were measured. Pressure was  
137 measured inside the plane while the temperature and RH sensor was located in the right wing of the  
138 plane. The location of plane was recorded by a GPS receiver.

## 139 **2.2 SMEAR II research station**

140 A research Station for Measuring Ecosystem-Atmospheric Relations (SMEAR) II in Hyytiälä,  
141 Southern Finland, was established in 1995 (see Hari and Kulmala, 2005). The station is equipped  
142 with several aerosol and gas instruments together with flux, irradiation and meteorological  
143 measurements. The long-term measurements give reliable and comprehensive knowledge about  
144 ambient conditions at a relatively clean coniferous forest site. The station includes ground-based  
145 measurements, tower measurements at the 35-m height above the ground level right above the  
146 canopy, and measurements conducted from a mast at different altitudes up to 128 m.

147 In this study, we mainly used particle data from the ground level as a reference data to which we  
148 compare our flight measurement data. The number concentrations in the size range of 1.5–3 nm were  
149 calculated from the difference between the measured total particle concentration at the 1.5 nm cut-  
150 off size (from the PSM) and total concentration at the 3 nm cut-off size (from DMPS). The distance  
151 between the PSM and DMPS is vertically a few meters and horizontally a few tens of meters, which  
152 causes some uncertainties in 1.5–3 nm particle number concentrations, especially during poorly-  
153 mixed BL times in the morning when the two instruments do not always measure the same air mass.

154 The sensible heat flux (SHF) was measured at the at 23-m height, and we used these data to get  
155 qualitative information on the strength of vertical mixing in the measured air masses.

## 156 **2.3 Data analysis**

157 The particle number concentration in the size range of 1.5–3 nm was calculated as the difference of  
158 the total particle concentrations measured with the PSM and uCPC on board the Cessna. The cut-off  
159 sizes of these instruments were 1.5 nm and 3 nm. The cut-off size of the SMPS was 10 nm. The  
160 number concentration in the size range of 3–10 nm was calculated as the difference in the total particle  
161 number concentrations measured with uCPC and SMPS.

162 Total particle number concentrations measured on board the Cessna were first converted into standard  
163 temperature and pressure conditions (STP, 273.15K, 100 kPa) and then were corrected with the  
164 maximum detection efficiency of the instrument based on laboratory calibrations. The maximum  
165 detection efficiency of the PSM used in airborne measurement was 0.75 and that of uCPC was 0.99.  
166 The maximum detection efficiencies of the PSMs used at the station were 0.8. Finally, the particle  
167 number concentrations were corrected with respect to diffusional losses in the inlet part (Fig. 1) and  
168 inside the sampling lines on the plane, assuming a constant correction factor for each size bin. The  
169 ground and tower data were assumed to have negligible inlet line losses because of core sampling  
170 (Kangasluoma et al., 2016). The correction factor for the inlet part was 0.716 for 1.5–3 nm particles  
171 and 0.720 for 3–10 nm particles based on simulation results using COMSOL Multiphysics software.  
172 Penetration efficiencies through the sampling lines were 0.70 and 0.88 in the size ranges of 1.5–3 nm  
173 and 3–10 nm, respectively.

174 All the results presented here are reported vertically as meters above the ground level, and all the data  
175 were collected from within a distance of 30 km from the SMEAR II station in Hyytiälä. A typical  
176 measurement flight includes a linear ascent from 100–200 m (a.g.l.) up to the FT region, 2500–3500  
177 m, and a descent back near to the canopy top level.

178 In this study, we analysed altogether 53 measurement profiles during 18 days. The flights were  
179 conducted during three measurement campaigns: May-June 2015, August 2015 and April-May 2017,  
180 either in the morning (7:00–12:00, UTC+2) or in the afternoon (12:00–15:00) time. The days were  
181 classified as event, non-event or undefined days based on the NPF event classification method by Dal  
182 Maso et al. (2005).

183 Well-mixed boundary layers are capped by a stable layer. The boundary layer height (BLH) was  
184 visually estimated from the in-situ measurements onboard the Cessna aircraft for each vertical  
185 measurement profile. The BLH was estimated from minimum vertical gradient in H<sub>2</sub>O and RH, and  
186 maximum vertical gradient in the potential temperature. The estimated BLH was evaluated visually  
187 with Doppler lidar profiles when possible (due to very low lidar signal-to-noise ratio in the clean-air

188 environment), and was found to agree very well. When the sun is rising, the mixing of air mass starts  
189 from near the ground, and aerosol particles originating from surface get mixed upwards within the  
190 rising mixed layer. Inside the mixing layer, higher concentrations of H<sub>2</sub>O are sometimes seen when  
191 the turbulence mixes up the moisture from the surface. CO<sub>2</sub> tends to be higher in the morning  
192 boundary layer due to respiration and decreases in the residual layer. The vertical profile of the  
193 potential temperature is almost constant in the surface mixed layer and rapidly increases with an  
194 increasing altitude under stable conditions.

195

## 196 **2.4 Uncertainties**

197 As described above, all the results were converted into standard temperature and pressure (STP, 100  
198 kPa, 273.15K) conditions and corrected for the instrumental maximum detection efficiency and line  
199 losses according to the laboratory characterizations of the flight setup. However, there are several  
200 factors causing uncertainties in the measured concentrations. The flight speed, main flow rate, air  
201 pressure, relative humidity and temperature are changing rapidly during a flight, which can cause  
202 variations in the inlet flows and the performance of the instruments. It is poorly known how the uCPC  
203 and PSM behave under quickly varying operational conditions. The reduced pressure at high altitudes  
204 may change the maximum detection efficiency and cut-off size of laminar flow CPCs (e.g. Zhang and  
205 Liu, 1991; Herrman and Wiedensohler, 2001). The pressure effect on the PSM cut-off size has been  
206 observed to be small ( $< 0.1$  nm until 60 kPa) compared to the uncertainty caused by a changing  
207 relative humidity and particle composition (Kangasluoma et al., 2016). We measured up to altitudes  
208 with the pressure going down to  $\sim 70$  kPa, which gives an uncertainty of  $\pm 5$  % for the aerosol flow  
209 rate of the CPC 3776, and thus directly to the concentrations, as shown by Takegawa et al. (2017),  
210 Fig 3. In addition, we compared the concentrations measured by PSM, uCPC and SMPS in the FT  
211 where the occurrence of small particles (below 10 nm, that has been under discussion in this paper)  
212 is very low. These concentrations matched well with each other, so we may assume that the pressure  
213 effect to the measured concentrations for any of the instruments was not significant in our study.

214 Because of the uncertainties in the instrument cut-off sizes, the true size range of the 1.5–3 nm  
215 concentration may vary with altitude and between different flights. This would also slightly affect the  
216 particle sampling losses, which were here assumed to be constant for the whole size range, although  
217 in reality there is a size dependency. Because of these uncertainties in the determined concentrations,  
218 we should focus on the relative behaviour of median values rather than absolute concentrations.

219

## 220 **3 Results and discussion**

221

222 The flight days were divided into event, non-event and undefined days based on the NPF event  
223 classification by Dal Maso et al. (2005). Based on this classification on the ground level, the vertical  
224 profiles of particles in the size ranges of 1.5–3 nm and 3–10 nm were studied separately in each type  
225 of days. During event and undefined days, we also looked at differences between the morning and  
226 afternoon times. The number of flights during non-event days is low (two vertical profiles), because  
227 cloudiness makes the operation of the aircraft impossible. Non-event days are mostly cloudy in  
228 Hyytiälä (Dada et al., 2017).

229 For the flight days, when we have comparable particle data from the ground station, we calculated  
230 the median values of 1.5–3 nm particle concentration both inside BL on board the Cessna and on the  
231 ground level. The boundary layer height was estimated for every vertical measurement profile.

### 232 **3.1 General features and vertical profiles**

233 The median values of particle concentrations, sensible heat flux (SHF), median of measurement  
234 height and estimated BLH was calculated for the 27 cases when comparable data were available at  
235 the SMEAR II station (Table 1). The values onboard aircraft (inside the BL) indicates here the  
236 observations on board Cessna, which means that the minimum limit for altitude was around 100 m  
237 from ground level. The values on the ground level were measured inside the forest canopy.

238 On average, we found that the concentration of 1.5–3 nm particles were higher onboard aircraft  
239 (inside the BL) ( $1400 \text{ cm}^{-3}$ ) than on the ground station level ( $1100 \text{ cm}^{-3}$ ) (hereafter referred to as  
240 ‘ground’). The observation of having somewhat lower concentrations of small particles at ground  
241 level is probably due to higher sinks of particles and their precursors inside the canopy compared  
242 with above-canopy air (Tammiet et al., 2006; Zha et al., 2018). The values were the highest on NPF  
243 event days ( $1500 \text{ cm}^{-3}$  onboard aircraft (inside the BL) and  $1300 \text{ cm}^{-3}$  on the ground) and undefined  
244 days ( $1450 \text{ cm}^{-3}$  onboard aircraft (inside the BL) and  $1130 \text{ cm}^{-3}$  on the ground) and clearly the lowest  
245 on non-event day both onboard aircraft (inside the BL) ( $890 \text{ cm}^{-3}$ ) and on the ground level ( $740 \text{ cm}^{-3}$ ).  
246 It should be noted that both of two non-event profiles were measured during the same afternoon  
247 in the spring of 2015.

248 The median BLH of all the profiles was 1400 m, being lower in the morning (1100 m) and higher  
249 during the afternoon flights (2000 m). Indicative of stronger vertical mixing, the median value of the



250 sensible heat flux (SHF) was the highest on the NPF event days, especially during the afternoon (286  
251  $\text{W m}^{-2}$ ).

252 Figure 2 shows the median vertical profiles of the total particle number concentration in the size  
253 ranges of 1.5–3 nm and 3–10 nm separately for the NPF event days, undefined days and one non-  
254 event day. The profiles typically contain data from 100 m up to 2700 m above the ground level. It is  
255 noticeable that the non-event profile consists of only two vertical profiles and that both of them were  
256 measured in the same afternoon. We found that airborne 1.5–3 nm particle concentrations were  
257 similar between the event and undefined days, whereas substantially lower concentrations were  
258 observed on non-event day. We also observed that during the event days there were clearly more 3–  
259 10 nm particles inside the BL (onboard aircraft) than during undefined days (Fig. 2a and 2b). The  
260 reason for this could be that during the undefined days the formation of sub-3 nm particles took place,  
261 yet the conditions were not suitable for the particle growth to larger sizes (see Buenrostro Mazon et  
262 al., 2009; Kulmala et al., 2013). Our findings are consistent with earlier observations of high sub-3  
263 nm particle concentrations in Hyytiälä on both event and undefined days compared with non-event  
264 days (Lehtipalo et al., 2009; Dada et al., 2017).

265 During the NPF event days, median, 25<sup>th</sup> and 75<sup>th</sup> percentiles show that the concentration of sub-3  
266 nm particles was relatively the highest right above the canopy top. This indicates that the sources of  
267 particles and their precursor vapors are near the ground level. During the undefined days, the origin  
268 of sub-3 nm particles was not necessarily at the ground level, as their concentration decreased right  
269 above the ground level (from 100 m to 200 m). In addition, reviewing the median values in Table 1,  
270 the concentration of 1.5–3 nm particles was observed to be higher inside the BL (onboard aircraft)  
271 during morning times of undefined days ( $2800 \text{ cm}^{-3}$ ) than during afternoon times ( $1150 \text{ cm}^{-3}$ ),  
272 oppositely to event days ( $1070 \text{ cm}^{-3}$  and  $3020 \text{ cm}^{-3}$ , respectively), which supports this hypothesis  
273 (Table 1). The concentrations of both sub-3 nm and 3–10 nm particles were very low during the non-  
274 event days and we did not observe any clear layers for these particles. However, it should be noted  
275 that our study included only two such profiles, since the flight measurements were not possible to  
276 conduct during non-event days due to meteorological conditions, especially cloudiness.

277 The measurement flights were conducted either in the morning (7:00–12:00, UTC+2) or in the  
278 afternoon (12:00–15:00). We studied the median vertical particle concentrations separately for those  
279 two times in order to estimate the effect of mixing strength on the vertical profile of particles on NPF  
280 event and undefined days. As expected based on observed SHF fluxes, we found that the  
281 concentrations of 1.5–3 nm particles inside the BL (onboard aircraft) were, on average, most  
282 homogenous vertically during the afternoons of the NPF event days (Fig. 3).

283 On NPF event days, we can see an interesting layer of 3–10 nm particles in the morning above the  
284 BL at 2400 m. From this layer, the particles can mix down into the evolving BL. A similar behavior  
285 is seen on undefined days, when the increase in concentration of 1.5–3 nm particles is observed in  
286 layer right below 2500 m in the morning and the particles are grown in size and mix downward until  
287 afternoon.

### 288 **3.2 Diurnal variation of particle concentration at different altitudes in the lower** 289 **atmosphere**

290 We studied the median diurnal variation of total particle concentration (all particles > 1.5 nm) and  
291 separately particle concentration in size range of 1.5–3 nm at different altitudes from around 100 m  
292 to 2700 m above the ground level around the SMEAR II station area. The study included 17 vertical  
293 measurement profiles during event days and 34 during undefined days. From Fig. 4a it can be seen  
294 that the total particle number concentration over all measurement profiles was the highest near the  
295 ground in the morning. The aerosol population mixed with cleaner air within the evolving BL after  
296 the morning, which led to a decreasing particle number concentration, whereas the concentration  
297 increased again towards the afternoon, presumably as a result of NPF. The highest particle number  
298 concentrations were observed at 11:30–14:30 inside the BL (onboard aircraft), which coincides with  
299 the peak time of NPF in Hyytiälä (Dada et al., 2018).

300 The sub-3 nm particle number concentrations (Fig. 4b) were the highest in the morning near the  
301 ground level, with a second maximum around the noon. Later in the afternoon, the sub-3 nm particle  
302 concentration was clearly lower, probably because these particles apparently grew efficiently to larger  
303 sizes and contributed significantly to the total particle concentration (Yli-Juuti et al., 2011). Both total  
304 particles and sub-3 nm particles had the highest concentrations near the ground level throughout the  
305 day, even though especially the total particle population seems to have been spread within the whole  
306 mixed layer.

307 Figure 4c shows the data availability for this analysis. It is noticeable that the number of data in each  
308 100 m-half-an-hour cell varies considerably. In addition, one intense NPF event day with strong  
309 particle formation in the early morning dominated the distribution due to the low number of flights at  
310 around 7:00–8:00. Most of the data were collected either during the morning (8:30–11:30) or  
311 afternoon (13:30–15:00). As we know, also the BLH, mixing of air and meteorological conditions  
312 can differ significantly even within one day, and especially so between the NPF event and undefined  
313 days.

### 314 **3.3 Case study – NPF in evolving BL**

315 The 13<sup>th</sup> of August 2015 was an intense NPF event day in Hyytiälä (Fig. 5a). During that day we  
316 conducted two measurement flights around the SMEAR II station and observed the particle  
317 concentration in size range of 1.5–3 nm to follow the development of BL and turbulent mixing (Fig.  
318 6a, 6c, 7a, 7c). During the first measurement flight at 7:30–9:00, we observed a clear layer of 3–10  
319 nm particles near the FT region above 2300 m. These particles were mixed down before the afternoon  
320 flight, as this population was not anymore observed during that flight. The negative (downwards)  
321 particle flux at SMEAR II after 12:00 supports this hypothesis (Fig. 5b).

322 The estimated BLH was ~500–700 meters during the first flight in the morning and had risen up to  
323 1500–1700 meters until afternoon flight. Below the FT, the vertical variation of the 1.5–3 nm particle  
324 concentration was larger compared to the stable conditions in FT. The median of concentration of  
325 1.5–3 nm particles inside the BL (onboard aircraft) decreased from the morning flight (7300 cm<sup>-3</sup>  
326 during the ascent and 6300 cm<sup>-3</sup> during the descent, Fig. 6a and 6c) to the afternoon flight (~2500 cm<sup>-3</sup>  
327 <sup>3</sup>, Fig. 7a and 7c), whereas 3–10 nm particles seemed to behave in an opposite manner (350 cm<sup>-3</sup>, 200  
328 cm<sup>-3</sup>, 850 cm<sup>-3</sup> and 1450 cm<sup>-3</sup>). The sub-3 nm particle concentrations were clearly higher inside the  
329 BL (onboard aircraft) than in the FT, and the concentration increased towards the ground. This is  
330 consistent with organic vapors, emitted from the ground vegetation, participating in NPF and growth  
331 (Kulmala et al., 2013; Ehn et al., 2014).

332

## 333 **4 Conclusions**

334

335 Small 1.5–3 nm particles were observed inside the convective BL on-board a Cessna aircraft. On  
336 average, the highest concentrations of sub-3 nm particles were found during NPF event mornings  
337 above the forest canopy top. This points towards the forest being an important source of the precursor  
338 vapors for newly formed particles. Due to the convective mixing inside BL, small particles near the  
339 ground started to mix up while sub-10 nm particles mixed down from the FT region. Strong vertical  
340 mixing was more typical for the NPF event days than for the undefined and non-event days, especially  
341 during the afternoon. The concentration of sub-3 nm particles was clearly higher inside the BL  
342 (onboard aircraft) on both NPF event days and undefined days compared with one non-event day, but  
343 their vertical variation was somewhat different, reflecting the different mixing conditions. The event  
344 days also showed a clear increase of 3–10 nm particles in the afternoon, which was missing on  
345 undefined days when the NPF process had been interrupted.

346 We found that airborne and on-ground median concentrations of sub-3 nm particles were mostly in  
347 good agreement. Some differences still existed, which can be explained by poor vertical mixing of  
348 air, changes in air mass origins and regional variations. The concentrations of sub-3 nm particles on  
349 the ground were, on average, somewhat lower than airborne observations, which indicates a higher  
350 sink for these particles inside the forest canopy.

351 This study increases our understanding of the first steps of atmospheric NPF inside the whole BL and  
352 the connections between atmospheric mixing and NPF. The next step would be to investigate different  
353 formation pathways in more detail. To achieve this, it would be important to find out also the chemical  
354 composition of particles above the ground level so that we could assess more specifically the possible  
355 sources of the precursor gases. In addition, the contribution of mesoscale convection-induced  
356 movement, like roll vortices, to NPF is currently under investigation.

357

#### 358 **Author contribution**

359 Katri Leino, Janne Lampilahti and Riikka Väänänen designed the experiments and installed the  
360 instrumentation. Frans Korhonen, Erkki Siivola, Heikki Laakso and Teemu Matilainen took part to  
361 the installing and instrumentation rack developments. The measurement flights carried out by Katri  
362 Leino, Janne Lampilahti, Riikka Väänänen, Pyry Poutanen, Antti Manninen, Lubna Dada, Anna  
363 Nikandrova and Daniela Wimmer. Stephany Buenrostro Mazon made NPF event forecasts. Pasi  
364 Aalto, Lauri Ahonen, Juha Kangasluoma, Petri Keronen and Joonas Enroth helped with  
365 instrumentation calibrations. Katri Leino prepared the manuscript with contributions from all co-  
366 authors.

367

#### 368 **Acknowledgements**

369 This work was supported by the European Research Council via ERC-Advanced Grant ATM-GTP  
370 (742206), the European Commission via projects H2020-INFRAIA-2014-2015 project ACTRIS-2  
371 (Aerosols, Clouds, and Trace gases Research InfraStructure), H2020 research and innovation  
372 programme under grant agreement No 689443 (ERAPLANET) via project iCUPE (Integrative and  
373 Comprehensive Understanding on Polar Environments), FP7 project BACCHUS (Impact of Biogenic  
374 versus Anthropogenic emissions on Clouds and Climate: towards a Holistic UnderStanding, FP7-  
375 603445), Academy of Finland via Centre of Excellence in Atmospheric Sciences (272041) and  
376 NanoBiomass (307537).

377

378 **References**

- 379 Boy, M., Hellmuth, O., Korhonen, H., Nilsson, E.D., Revelle, D., Turnipseed, A., Arnold, F. and  
380 Kulmala, M.: MALTE – model to predict new aerosol formation in the lower troposphere,  
381 Atmos. Chem. Phys., 6, 4499–4517, <https://doi.org/10.5194/acp-6-4499-2006>, 2006.
- 382 Bianchi, F., Tröstl, J., Junninen, H., Frege, C., Henne, S., Hoyle, C. R., Molteni, U., Herrmann, E.,  
383 Adamov, A., Bukowiecki, N., Chen, X., Duplissy, J., Gysel, M., Hutterli, M., Kangasluoma, J.,  
384 Kontkanen, J., Kürten, A., Manninen, H. E., Münch, S., Peräkylä, O., Petäjä, T., Rondo, L.,  
385 Williamson, C., Weingartner, E., Curtius, J., Worsnop, D. R., Kulmala, M., Dommen, J., and  
386 Baltensperger, U.: New particle formation in the free troposphere: A question of chemistry and  
387 timing, Science, 352, 1109–1112, <https://doi.org/10.1126/science.aad5456>, 2016.
- 388 Buenrostro Mazon, S., Riipinen, I., Schultz, D.M., Valtanen, M., Dal Maso, M., Sogacheva, L.,  
389 Junninen, H., Nieminen, T., Kerminen, V.-M. and Kulmala, M.: Classifying previously  
390 undefined days from eleven years of aerosol-particle-size distribution data from the SMEAR II  
391 station, Hyytiälä, Finland, Atmos. Chem. Phys., 9, 667–676, [https://doi.org/10.5194/acp-9-667-](https://doi.org/10.5194/acp-9-667-2009)  
392 [2009](https://doi.org/10.5194/acp-9-667-2009), 2009.
- 393 Chen, H., Hodshire, A.L., Ortega, J., Greenberg, J., McMurry, P.H., Carlton, A.G., Pierce, J.R.,  
394 Hanson, D.R. and Smith, J.N.: Vertically resolved concentration and liquid water content of  
395 atmospheric nanoparticles at the US DOE Southern Great Plains site, Atmos. Chem. Phys.,  
396 18, 311–326, <https://doi.org/10.5194/acp-18-311-2018>, 2018.
- 397 Crumeyrolle, S., Manninen, H., Sellegri, K., Roberts, G., Gomes, L., Kulmala, M., Weigel, R., Laj,  
398 P. and Schwarzenboeck, A.: New particle formation events measured on board the ATR-42  
399 aircraft during the EUCAARI campaign, Atmos. Chem. Phys., 10, 14,  
400 <https://doi.org/10.5194/acp-10-6721-2010>, 2010.
- 401 Dada, L., Paasonen, P., Nieminen, T., Buenrostro Mazon, S., Kontkanen, J., Peräkylä, P., Lehtipalo,  
402 K., Hussein, T., Petäjä T., Kerminen, V.-M., Bäck, J. and Kulmala, M.: Long-term analysis of  
403 clear-sky new particle formation events and nonevents in Hyytiälä, Atmos. Chem. Phys., 17,  
404 6227–6241, <https://doi.org/10.5194/acp-17-6227-2017>, 2017.
- 405 Dada L., Chellapermal R., Buenrostro Mazon S., Paasonen P., Lampilahti J., Manninen H. E.,  
406 Junninen H., Petäjä T., Kerminen V.-M. and Kulmala M.: Refined classification and  
407 characterization of atmospheric new-particle formation events using air ions, Atmos. Chem.  
408 Phys. 18, 17883–17893, <https://doi.org/10.5194/acp-18-17883-2018>, 2018.

409 Dal Maso, M., Kulmala, M., Riipinen, I., Wagner, R., Hussein, T., Aalto, P.P. and Lehtinen, K.E.J.:  
410 Formation and growth of fresh atmospheric aerosols: eight years of aerosol size distribution  
411 data from SMEAR II, Hyytiälä, Finland, *Boreal Environ. Res.*, 10, 323–336, 2005.

412 Ehn, M., Thornton, J. A., Kleist, E., Sipilä, M., Junninen, H., Pullinen, I., Springer, M., Rubach, F.,  
413 Tillmann, R., Lee, B., Lopez-Hilfiker, F., Andres, S., Acir, I.-H., Rissanen, M., Jokinen, T.,  
414 Schobesberger, S., Kangasluoma, J., Kontkanen, J., Nieminen, T., Kurtén, T., Nielsen, L. B.,  
415 Jørgensen, S., Kjaergaard, H. G., Canagaratna, M., Maso, M. D., Berndt, T., Petäjä, T., Wahner,  
416 A., Kerminen, V.-M., Kulmala, M., Worsnop, D. R., Wildt, J. and Mentel, T. F.: A large source  
417 of low-volatility secondary organic aerosol, *Nature*, 506(7489), 476–479,  
418 <https://doi.org/10.1038/nature13032>, 2014.

419 Hari P. and Kulmala M.: Station for Measuring Ecosystem-Atmosphere Relations (SMEAR II),  
420 *Boreal Environ. Res.*, 10, 315–322, 2005.

421 Hermann, M. and Wiedensohler, A.: Counting efficiency of condensation particle counters at low-  
422 pressures with illustrative data from the upper troposphere, *J. Aerosol Sci.*, 32, 8, 975–991,  
423 [https://doi.org/10.1016/S0021-8502\(01\)00037-4](https://doi.org/10.1016/S0021-8502(01)00037-4), 2001.

424 Kangasluoma, J., Franchin, A., Duplissy, J., Ahonen, L., Korhonen, F., Attoui, M., Mikkilä, J.,  
425 Lehtipalo, K., Vanhanen, J., Kulmala, M. and Petäjä, T.: Operation of the Airmodus A11 nano  
426 Condensation Nucleus Counter at various inlet pressures and various operation temperatures,  
427 and design of a new inlet system, *Atmos. Meas. Tech.*, 9, 2977–2988,  
428 <https://doi.org/10.5194/amt-9-2977-2016>, 2016.

429 Kerminen, V.-M., V.-M., Petäjä, T., Manninen, H.E., Paasonen, P., Nieminen, T., Sipilä, M.,  
430 Junninen, H., Ehn, M., Gagné, S., Laakso, L., Riipinen, I., Vehkamäki, H., Kurten, T., Ortega,  
431 K., Dal Maso, M., Brus, D., Hyvärinen, A., Lihavainen, H., Leppä, J., Lehtinen, K.E.J., Mirme,  
432 A., Mirme, S., Hörrak, U., Berndt, T., Stratmann, F., Birmili, W., Wiedensohler, A., Metzger,  
433 A., Dommen, J., Baltensperger, U., Kiendler-Scharr, A., Mentel, T.F., Wildt, J., Winkler, P.M.,  
434 Wagner, P.E., Petzold, A., Minikin, A., Plass-Dülmer, C., Pöschl, U., Laaksonen, A. and  
435 Kulmala, M.: Atmospheric nucleation: highlights of the EUCAARI project and future  
436 directions, *Atmos. Chem. Phys.*, 10, 10829–10848, doi:10.5194/acp-10-10829-2010, 2010.

437 Kerminen V.-M., Chen, X., Vakkari, V., Petäjä, T., Kulmala, M. and Bianchi, F.: Atmospheric new  
438 particle formation: a review of field observations, *Environ. Res. Lett.*, 13,  
439 <https://doi.org/10.1088/1748-9326/aadf3c>, 2018.

- 440 Kulmala, M., Hämeri, K., Aalto, P.P., Mäkelä, J.M., Pirjola, L., Nilsson, E.D., Buzorius, G., Rannik,  
441 Ü., Dal Maso, M., Seidl, W., Hoffman, T., Janson, R., Hansson, H.-C., Viisanen, Y., Laaksonen,  
442 A. and O'Dowd, C.D.: Overview of the international project on biogenic aerosol formation in  
443 the boreal forest (BIOFAR), *Tellus*, 53, 4, <https://doi.org/10.1034/j.1600-0889.2001.530402.x>,  
444 2001.
- 445 Kulmala, M. and Kerminen, V.-M.: On the formation and growth of atmospheric nanoparticles,  
446 *Atmos. Res.*, 90, 2–4, 132–150, <https://doi.org/10.1016/j.atmosres.2008.01.005>, 2008.
- 447 Kulmala, M., Kontkanen, J., Junninen, H., Lehtipalo, K., Manninen, H.E., Nieminen, T., Petäjä, T.,  
448 Sipilä, M., Schobesberger, S., Rantala, P., Franchin, A., Jokinen, T., Järvinen, E., Äijälä, M.,  
449 Kangasluoma J., Hakala, J., Aalto, P.P., Paasonen, P., Mikkilä, J., Vanhanen, J., Aalto, J.,  
450 Hakola, H., Makkonen, U., Ruuskanen, T., Mauldin, R.L., Duplissy, J., Vehkamäki, H., Bäck,  
451 J., Kortelainen, A., Riipinen, I., Kurtén, T., Johnson, M.V., Smith, J.N., Ehn, M., Mentel, T.F.,  
452 Lehtinen, K.E.J., Laaksonen, A., Kerminen, V.-M. and Worsnop, D.R.: Direct observations of  
453 atmospheric aerosol nucleation, *Science*, 339, 943–946, DOI: 10.1126/science.1227385, 2013.
- 454 Kulmala, M., Vehkamäki, H., Petäjä, T., Dal Maso, M., Lauri, A., Kerminen, V.-M., Birmili, W. and  
455 McMurry, P.H.: Formation and growth rates of ultrafine atmospheric particles: A review of  
456 observations, *J. Aerosol Sci.*, 35, 143–176, <https://doi.org/10.1016/j.jaerosci.2003.10.003>,  
457 2004.
- 458 Laakso, L., Gronholm, T., Kulmala, L., Haapanala, S., Hirsikko, A., Lovejoy, E. R., Kazil, J., Kurten,  
459 T., Boy, M., Nilsson, E. D., Sogachev, A., Riipinen, I., Stratmann, F. and Kulmala, M.: Hot-air  
460 balloon as a platform for boundary layer profile measurements during particle formation, *Boreal*  
461 *Environ. Res.*, 12, 279–294, 2007.
- 462 Lauros, J., Sogachev, A., Smolander, S., Vuollekoski, H., Sihto, S.-L., Mammarella, I., Laakso, L.,  
463 Rannik, Ü. and Boy, M.: Particle concentration and flux dynamics in the atmospheric boundary  
464 layer as the indicator of formation mechanism, *Atmos. Chem. Phys.*, 11, 5591–5601,  
465 <https://doi.org/10.5194/acp-11-5591-2011>, 2011.
- 466 Lehtipalo, K., Sipilä, M., Riipinen, I., Nieminen, T. and Kulmala, M.: Analysis of atmospheric neutral  
467 and charged molecular clusters in boreal forest using pulse-height CPC, *Atmos. Chem. Phys.*,  
468 9, 4177–4184, <https://doi.org/10.5194/acp-9-4177-2009>, 2009.

469 Mirme, S., Mirme, A., Minikin, A., Petzold, A., Hörrak, U., Kerminen, V.-M. and Kulmala, M.:  
470 Atmospheric sub-3 nm particles at high altitudes, *Atmos. Chem. Phys.*, 10, 437–451,  
471 doi:10.5194/acp-10-437-2010, 2010.

472 O’Dowd, C., Yoon, Y., Junkermann, W., Aalto, P., Kulmala, M., Lihavainen, H., and Viisanen, Y.:  
473 Airborne measurements of nucleation mode particles II: boreal forest nucleation events, *Atmos.*  
474 *Chem. Phys.*, 9, doi:10.5194/acp-9-937-2009, 2009.

475 Platis, A., Altstädter, B., Wehner, B., Wildmann, N., Lampert, A., Hermann, M., Birmili, W. and  
476 Bange, J.: An observational case study on the influence of atmospheric boundary-layer  
477 dynamics on new particle formation, *Boundary-Layer Meteorol.*, 158, 1, 67–92,  
478 <https://doi.org/10.1007/s10546-015-0084-y>, 2016.

479 Rannik, Ü., Petäjä, T., Buzorius, G., Aalto, P., Vesala, T. and Kulmala, M.: Deposition Velocities of  
480 Nucleation Mode Particles into a Scots Pine Forest, *Environ. Chem. Phys.*, 22, 97–102, 2000.

481 Schobesberger, S., Väänänen, R., Leino, K., Virkkula, A., Backman, J., Pohja, T., Siivola, E.,  
482 Franchin, A., Mikkilä, J., Paramonov, M., Aalto, P. P., Krejci, R., Petaja, T. and Kulmala, M.:  
483 Airborne measurements over the boreal forest of southern Finland during new particle  
484 formation events in 2009 and 2010, *Boreal Environ. Res.*, 18, 145–163, 2013.

485 Siebert, H., Stratmann, F. and Wehner, B.: First observations of increased ultrafine particle number  
486 concentrations near the inversion of a continental planetary boundary layer and its relation to  
487 ground-based measurements, *Geophys. Res. Lett.*, 31, 9, 2004.

488 Stull, R. B.: An introduction to boundary layer meteorology, Springer Science & Business Media,  
489 2012.

490 Takegawa, N., Iida, K. and Sakurai, H.: Modification and laboratory evaluation of a TSI ultrafine  
491 condensation particle counter (Model 3776) for airborne measurements, *Aerosol Sci. Tech.*, 51,  
492 2, 235–245, <https://doi.org/10.1080/02786826.2016.1261990>, 2017.

493 Tammet, H., Hörrak, U., Laakso, L. and Kulmala, M.: Factors of air ion balance in a coniferous forest  
494 according to measurements in Hyytiälä, Finland, *Atmos. Chem. Phys.*, 6, 3377–3390,  
495 <https://doi.org/10.5194/acp-6-3377-2006>, 2006.

496 Vanhanen, J., Mikkilä, J., Lehtipalo, K., Sipilä, M., Manninen, H., Siivola, E., Petäjä, T., and  
497 Kulmala, M.: Particle size magnifier for nano-CN detection, *Aerosol Sci. Tech.*, 45, doi:  
498 10.1080/02786826.2010.547889, 2011.



- 499 Väänänen, R., Krejci, R., Manninen, H.E., Manninen, A., Lampilahti, J., Buenrostro Mazon, S.,  
500 Nieminen, T., Yli-Juuti, T., Kontkanen, J., Asmi, A., Aalto, P.P., Keronen, P., Pohja, T.,  
501 O'Connor, E., Kerminen, V.-M., Petäjä, T. and Kulmala, M.: Vertical and horizontal variation  
502 of aerosol number size distribution in the boreal environment, *Atmos. Chem. Phys. Discuss.*,  
503 doi:10.5194/acp-2016-556, 2016.
- 504 Wehner, B., Siebert, H., Stratmann, F., Tuch, T., Wiedensohler, A., Petäjä, T., Dal Maso, M. and  
505 Kulmala, M.: Horizontal homogeneity and vertical extent of new particle formation events,  
506 *Tellus*, 59, 3, 362–371, <https://doi.org/10.1111/j.1600-0889.2007.00260.x>, 2007.
- 507 Wehner, B., Wehner, F., Ditas, F., Shaw, R.A., Kulmala, M. and Siebert, H.: Observations of new  
508 particles formation in enhanced UV irradiance zones near cumulus clouds, *Atmos. Chem.*  
509 *Phys.*, 15, 11701–11711, <https://doi.org/10.5194/acp-15-11701-2015>, 2015.
- 510 Wehner, B., Siebert, H., Ansmann, A., Ditas, F., Seifert, P., Stratmann, F., Wiedensohler, A.,  
511 Apituley, A., Shaw, R., and Manninen, H. E.: Observations of turbulence-induced new particle  
512 formation in the residual layer, *Atmos. Chem. Phys.*, 10, 4319–4330,  
513 <https://doi.org/10.5194/acp-10-4319-2010>, 2010.
- 514 Yli-Juuti, T., Nieminen, T., Hirsikko, A., Aalto, P.P., Asmi, E., Hörrak, U., Manninen, H.E.,  
515 Patokoski, J., Dal Maso, M., Petäjä, T., Rinne, J., Kulmala, M. and Riipinen, I.: Growth rates  
516 of nucleation mode particles in Hyytiälä during 2003–2009: variation with particles size,  
517 season, data analysis method and ambient conditions, *Atmos. Chem. Phys.*, 11, 12865–12886,  
518 <https://doi.org/10.5194/acp-11-12865-2011>, 2011.
- 519 Zha, Q., Yan, C., Junninen, H., Riva, M., Sarnela, N., Aalto, J., Quéléver, L., Schallhart, S., Dada,  
520 L., Heikkinen, L., Peräkylä, O., Zou, J., Rose, C., Wang, Y., Mammarella, I., Katul, G., Vesala,  
521 T., Worsnop, D.R., Kulmala, M., Petäjä, T., Bianchi, F. and Ehn, M.: Vertical characterization  
522 of highly oxygenated molecules (HOMs) below and above a boreal forest canopy, *Atmos.*  
523 *Chem. Phys.*, 18, 17437–17450, <https://doi.org/10.5194/acp-18-17437-2018>, 2018.
- 524 Zhang, Z. Q. and Liu, B. Y. H.: Performance of Tsi 3760 Condensation Nuclei Counter at Reduced  
525 Pressures and Flow-Rates, *Aerosol Sci. Tech.*, 15, 228–238,  
526 <https://doi.org/10.1080/02786829108959530>, 1991.

527 **Tables**

528 Table 1. Numerical statistics about boundary layer height (BLH) and sensible heat flux (SHF)  
 529 indicating the mixing of air mass, and concentrations of 1.5–3 nm particles together with median  
 530 measurement heights during measurement flights in 2015 and 2017. The morning flights have been  
 531 conducted between 7:00–12:00 o'clock and afternoon flights at 12:00–15:00 o'clock. The low  
 532 number of flights during non-event days is caused by the cloudiness which makes the operation of  
 533 the aircraft impossible.

	Number of flight profiles when compara ble data from ground level were available	Median conc. (1.5–3 nm) inside BL onboard Cessna [ $\text{cm}^{-3}$ ]	Median conc. (1.5–3 nm) on ground level [ $\text{cm}^{-3}$ ]	Median BLH [m]	Median SHF [ $\text{W m}^{-2}$ ]	Median height [m a.g.l.]
All days	27	1404	1104	1400	192.3	722
morning	13	1995	888	1100	174.6	726
afternoon	14	1232	1251	2000	220.5	720
Events	9	1509	1300	1250	200	228
morning	5	1066	950	800	154.5	228
afternoon	4	3019	1435	1550	285.8	334
Undefined	16	1450	1129	1450	180.7	732
morning	8	2793	838	1200	182.6	728
afternoon	8	1149	1169	2000	178.7	736
Non-events	2	887	744	2000	162.3	868
morning	-	-	-	-	-	-
afternoon	2	887	744	2000	162.3	868

534

535

536

537 **Figures**

538

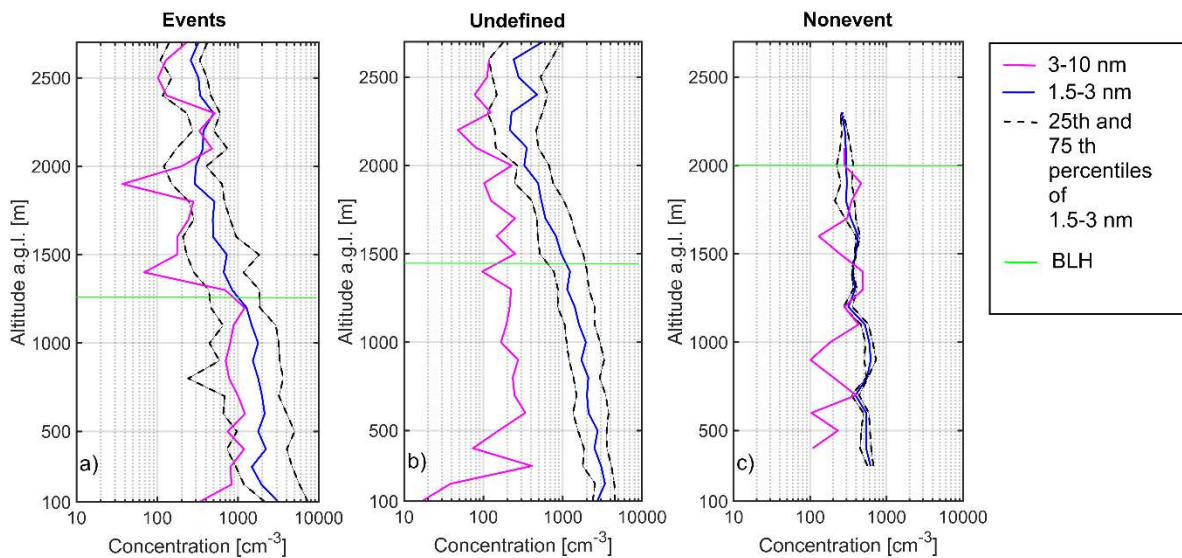
539



540

541 Figure 1. Instrumentation rack was installed inside the cabin (on the left) and the sample air for the  
542 instrumentation was taken from a steel tube at 50 cm distance from the fuselage of the plane (on the  
543 right). The main instruments (ultrafine-CPC, PSM and SMPS) are shown in figure.

544

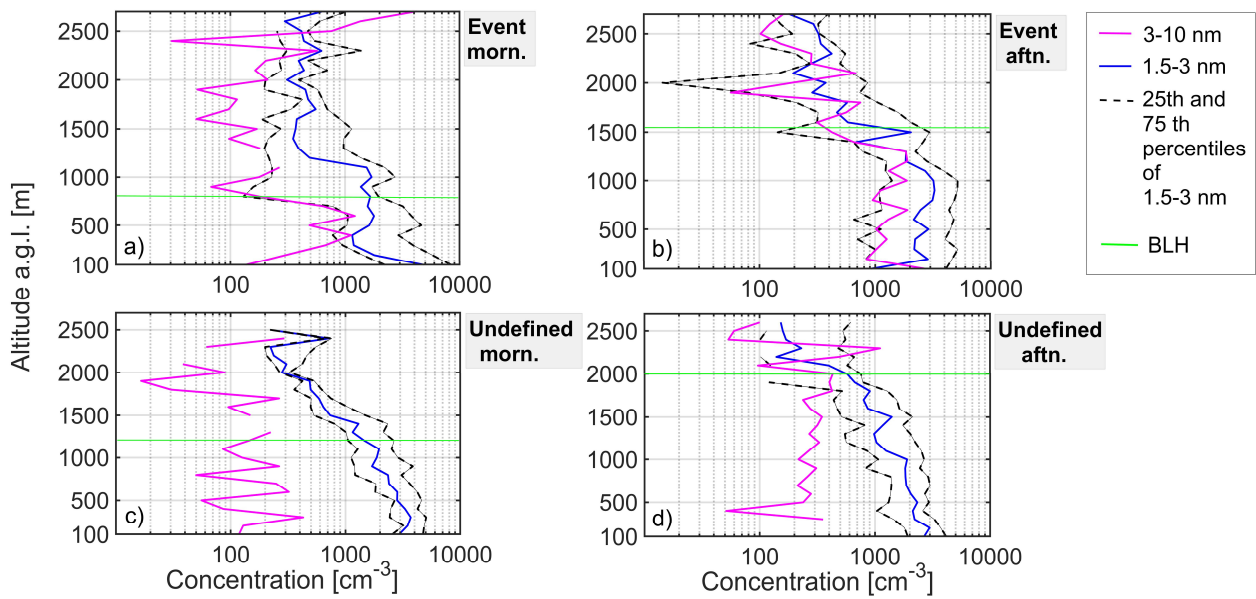


545

546

547 Figure 2. All day median particle concentrations in two size ranges, 3–10 nm (pink) and 1.5–3 nm  
548 (blue) and 25- and 75-percentiles (dashed lines) of the 1.5–3 nm particle concentration, as a  
549 function of altitude over 17 event day (a), 34 undefined day (b) and 2 non-event day afternoon  
550 profiles (c). The concentrations were calculated from the differences between three instruments  
551 (PSM, uCPC and SMPS) at different cut-off sizes: 1.5 nm, 3 nm and 10 nm, respectively. The data  
552 were collected from near (< 30 km) to SMEAR II station during spring and August flight  
553 measurement campaigns in 2015 and spring campaign 2017. Median boundary layer heights are  
554 marked by green lines.

555



556

557 Figure 3. Median concentrations in two size ranges (1.5–3 nm and 3–10 nm) and 25- and 75-  
 558 percentiles of 1.5–3 nm particle concentration over measurement profiles during event and  
 559 undefined days separately for morning (a, c) (7:00–12:00 o'clock) and afternoon (b, d) (12:00–  
 560 15:00 o'clock) times. The median vertical profiles were defined over 9 event morning, 8 event  
 561 afternoon, 18 undefined morning and 16 undefined afternoon profiles. Median boundary layer  
 562 heights are marked by green lines.

563

564

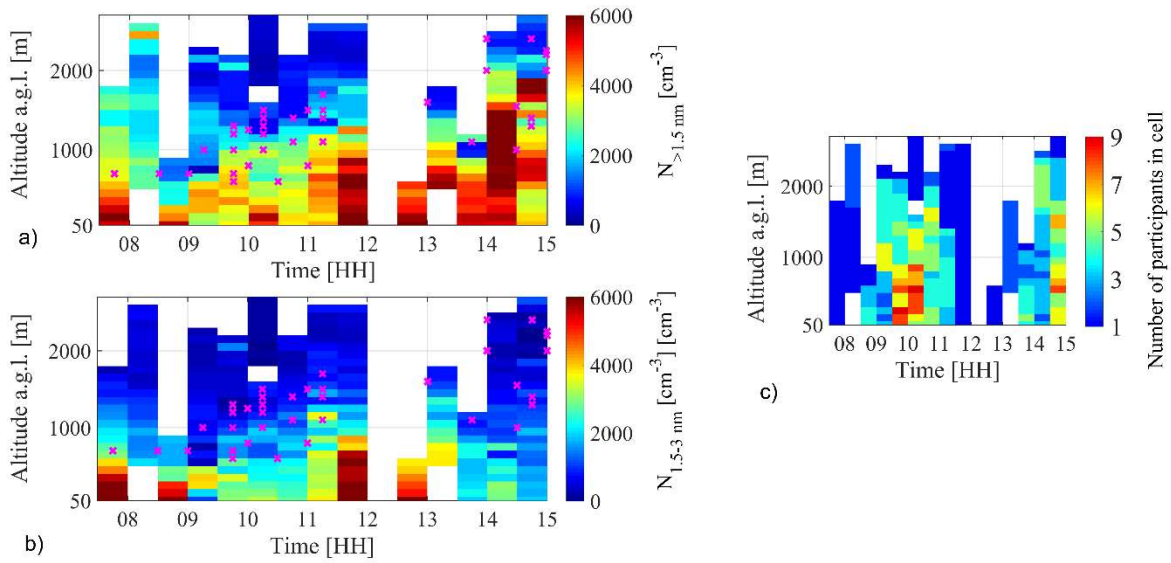
565

566

567

568

569



570

571

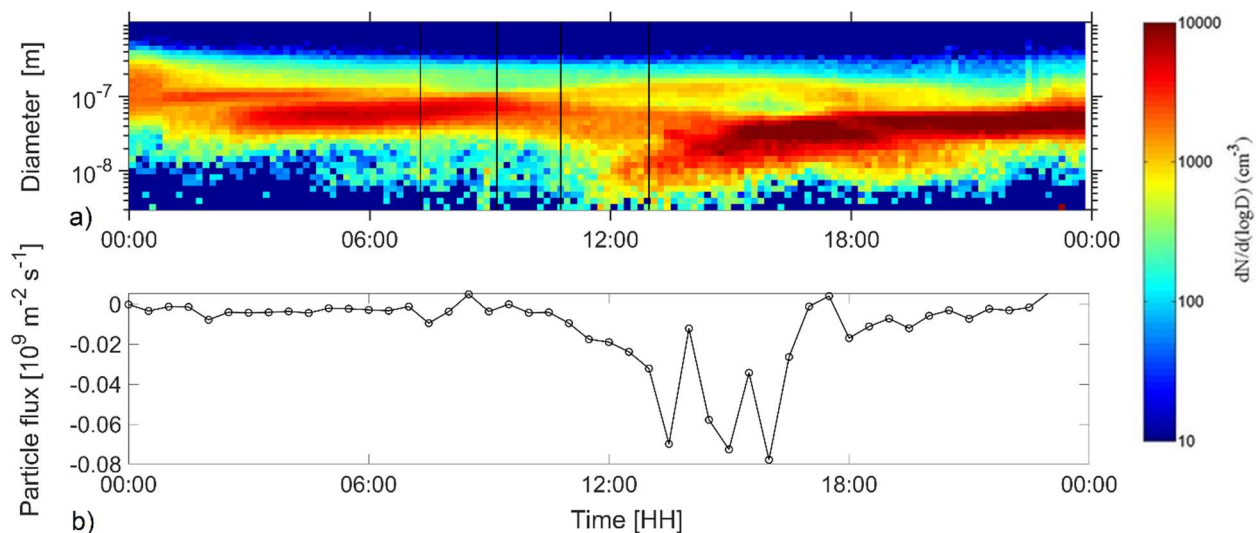
572 Figure 4. Panel a) shows median total particle number concentration at different altitudes calculated  
 573 over 51 measurement flight profiles (17 event day and 34 undefined day profiles) during 2015  
 574 spring and August and 2017 spring campaigns in 30 km maximum distance from SMEAR II  
 575 station. The total particle number concentration was measured with PSM with the cut-off size of 1.5  
 576 nm. Colour scale indicates total number concentration. Panel b) shows median particle number  
 577 concentration in the size range of 1.5–3 nm at different altitudes. The value is defined as difference  
 578 of total number concentrations with different cut-off sizes; PSM (1.5 nm) and uCPC (3 nm). Panel  
 579 c) shows the number of data points in each cell of figures a-b). Estimated boundary layer heights are  
 580 marked as crosses in figures a-b) over flight profiles. Each cell includes the median value of all  
 581 measurement points inside the 100 m bin and half-an-hour.

582

583

584

585



586

587 Figure 5. New particle formation event at SMEAR II station in Hyttiälä on 13<sup>th</sup> August 2015. Panel  
 588 a) shows the number size distribution measured by Differential Mobility Particle Sizer at ground  
 589 level inside the forest canopy. Start and end times of two measurement flights were marked by  
 590 vertical lines in figure. Panel b) shows the particle flux measured at 23 m above ground level at the  
 591 station. Negative particle flux indicates particles flux downwards.

592

593

594

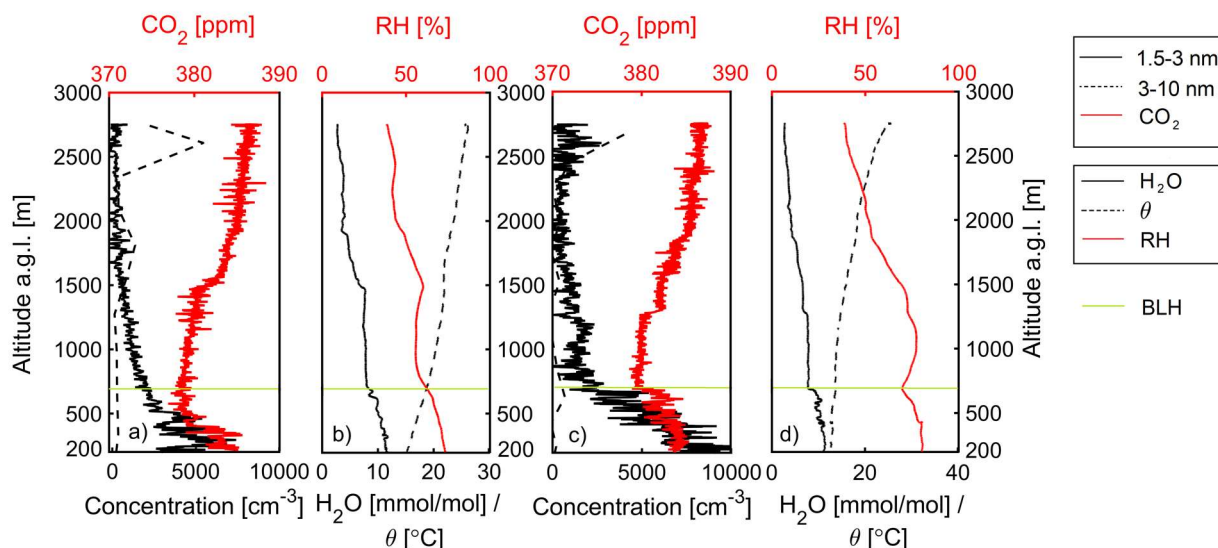
595

596

597

598

599

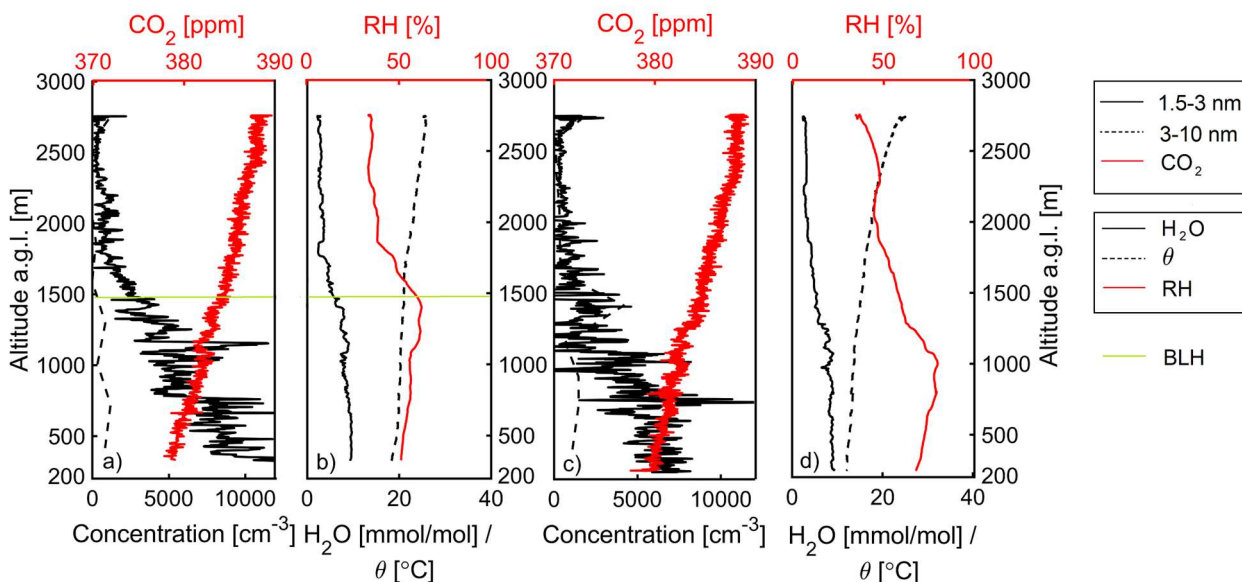


600

601 Figure 6. Vertical profiles during the first measurement flight at 7:30–9:00 a.m. on 13<sup>th</sup> August  
 602 2015 (marked in Fig 5). Panels a, b) show data from the ascent and c, d) from the descent. Figures  
 603 a) and c) show the number concentration of 1.5–3 nm (black solid line) and 3–10 nm (dashed line)  
 604 particles and the carbon dioxide concentration (red). Panels b) and d) show water vapor  
 605 concentration (black), relative humidity (red) and potential temperature (dashes line) profiles. The  
 606 green line is the estimated boundary layer height.

607

608



609

610 Figure 7. Measurement profiles like in the previous figure, but during the second measurement  
 611 flight on 13<sup>th</sup> August 2015 at 11:00 a.m. – 12:45 p.m.

612